Modeling and Fault Ride-Through Control Strategy for Grid-Supporting Photovoltaic-Based Microgrids

Innocent Ewean Davidson*‡, Elutunji Buraimoh *,

* African Space Innovation Centre (ASIC), Cape Peninsula University of Technology, Bellville, Cape Town 7535, South Africa

(davidsoni@cput.ac.za, elutunji@gmail.com)

‡ Corresponding Author, Bellville, Cape Town 7535, South Africa, Tel: +27 73 932 9525,

Fax: +27 73 932 9525, davidsoni@cput.ac.za

Received: 27.03.2023 Accepted:24.06.2023

Abstract- This research paper presents a detailed modeling approach for a grid-supporting microgrid system based on photovoltaic (PV) technology. The study encompasses the development of a comprehensive model that accurately represents the dynamic behavior of the microgrid components, including PV arrays, DC-DC converters, DC-AC inverters, and the grid interface. Emphasis is placed on incorporating fault ride-through control techniques to enhance the microgrid's resilience and maintain an uninterrupted power supply during grid disturbances. The modeling process involves capturing the electrical characteristics and interactions among various system components using suitable mathematical equations and control algorithms. Special attention is given to accurately representing the PV arrays' output characteristics and the converter and inverter dynamics. The resulting model provides a reliable platform for studying the system's behavior under different operating conditions, including normal grid operation and fault scenarios. Furthermore, the study addresses the implementation of fault ride-through control mechanisms to ensure the microgrid's stability and ability to ride through grid faults. Various control strategies, such as voltage and current control, droop control, and active/reactive power control, are investigated and integrated into the system model. These control techniques enable the microgrid to autonomously regulate its power output and maintain stable voltage and frequency levels during grid disturbances, thereby enhancing the microgrid's reliability and grid-supporting capabilities. The proposed modeling and fault ride-through control strategies are evaluated through extensive simulations and analysis. The microgrid's performance under different fault scenarios, including voltage sags, voltage swells, and grid disconnections, is thoroughly assessed to validate the effectiveness of the implemented control strategies. Thus, this study provides valuable insights into a PV-based grid-supporting microgrid's modeling and control aspects, demonstrating the feasibility and effectiveness of fault ride-through control techniques. The findings contribute to the advancement of microgrid technologies and support the integration of renewable energy sources into the existing power grid infrastructure.

Keywords: Photovoltaics, Smart microgrid, Secondary control scheme, Renewable Energy Sources.

1. Introduction

Globally, there has been a significant increase in the adoption and integration of renewable energy (RE) based distributed resources into electrical power networks. This integration is facilitated by using microgrids as intermediaries, which serve as localized systems that generate, distribute, and store electricity. In parallel, power electronic-based converters have emerged as a crucial technological solution for interfacing these renewable energy sources with the grid and providing enhanced control flexibility. Among the various types of power electronic converters, switch-model power electronic inverters have become the core technology for enabling the grid integration of RE intermittent DC power into traditional AC grids [1]. These inverters are designed to convert direct current (DC) power generated by renewable sources such as solar panels or wind turbines into alternating current (AC) power compatible with the existing AC grid infrastructure.

The use of switch-model power electronic inverters offers several advantages in grid integration. Firstly, they

provide efficient and precise control over the conversion process, allowing for optimal power flow management and voltage regulation. This control flexibility enables smooth and reliable integration of intermittent renewable energy sources, which fluctuate in their power output due to weather conditions or other factors. Furthermore, switch-model power electronic inverters facilitate the seamless integration of distributed energy resources (DERs) into the power grid. DERs encompass various forms of decentralized renewable energy generation, such as rooftop solar panels or small-scale wind turbines [2]. By converting the DC power generated by these DERs into AC power compatible with the grid, the switch-model inverters enable the DERs to contribute to the overall energy supply and support the grid during peak demand periods.

In addition to their integration capabilities, switch-model power electronic inverters offer enhanced grid stability and resilience. They can actively respond to grid disturbances and contribute to voltage and frequency regulation, thereby improving the overall reliability of the power system. Moreover, these inverters can support the grid by providing ancillary services, such as reactive power compensation or voltage support, further enhancing grid stability. Thus, the utilization of switch-model power electronic inverters has played a crucial role in enabling the integration of renewable energy sources into traditional AC grids. This technology has paved the way for the widespread deployment of microgrids and the effective utilization of distributed energy resources, ultimately contributing to the global transition towards a more sustainable and resilient energy future [3].

Different DER architectures have been developed to cater to specific system sizes and applications, considering their unique qualities and requirements. In order to optimize the operation of power electronic interface inverters within these architectures, adequate modeling and selection of control parameters are essential. One common application is using DC-DC converters to interface a DC-based distributed generation (DG) source, such as photovoltaic (PV) panels, with the rest of the system, aiming to achieve maximum power extraction and stabilize the DC-link voltage. For instance, a double-stage PV system can be employed, where a DC-DC converter with maximum power point tracking (MPPT) control is utilized in conjunction with a DC-AC inverter. The primary purpose of the DC-DC converter in this configuration is to optimize the power output of the PV panels. It achieves this by continuously tracking and adjusting the operating point of the panels to ensure that they operate at their maximum power point (MPP) under varying environmental conditions. The MPPT control algorithm employed in the DC-DC converter enables efficient power extraction from the PV panels by dynamically adjusting the converter's operating parameters.

The output of the DC-DC converter, now at the desired voltage and power level, is then fed to the DC-AC inverter for further conversion into AC suitable for integration with the AC grid or local loads. The control of the DC-AC inverter is slightly modified to accommodate the specific requirements of the double-stage PV system. This modified control scheme ensures that the inverter operates in a coordinated manner with the DC-DC converter, allowing for efficient power transfer and grid synchronization. The overall system architecture, including the DC-DC converter with MPPT control and the modified control of the DC-AC inverter, enables effective utilization of the PV panels, maximizes the power output, and maintains the stability of the DC-link voltage. By employing advanced control algorithms and appropriate parameter selection, the operation of power electronic interface inverters in DER architectures can be enhanced, leading to improved system performance and increased energy efficiency [4].

Numerous studies have been conducted to investigate and optimize the performance of these DER architectures. These studies emphasize the importance of accurately modeling the components involved, such as the PV panels, DC-DC converter, and DC-AC inverter, to capture their dynamic behavior and interactions. Additionally, selecting appropriate control parameters and tuning them accordingly is crucial to achieving optimal performance and ensuring the system's reliable and stable operation. In summary, the selection and design of DER architectures are influenced by factors like system size and application requirements. The operation of power electronic interface inverters within these architectures can be enhanced through proper modeling and control parameter selection. The utilization of DC-DC converters in PV systems, coupled with MPPT control and modified control schemes for DC-AC inverters, exemplifies one approach to achieving maximum power extraction and stable operation in such systems. Continuous research and optimization efforts contribute to advancing the efficiency and effectiveness of these DER architectures and their associated control strategies [5].

Consequently, this study introduces the unique concept of integrating active power frequency and reactive power voltage droops for a solar-photovoltaic system to dynamically support the power grid by participating in frequency and voltage regulation. The paper's balance presents the simulation results to validate the models developed. This study adds a DC-DC converter to an inverter-based microgrid in grid-supporting mode. This reflects real DC source DER/DG dynamics, especially a double-stage Solar Photovoltaic system, as countries worldwide drive towards increasing RES use, especially in grid-synchronous operating conditions. Furthermore, the global capital and installation cost of PV panels continuously declines. However, the power conversion unit is inevitable for properly integrating the PV system. Consequently, the control system design for power electronic converters required for DC-DC and DC-AC conversions is critical to enhancing durability, reliability, and efficiency [6]. This study is not focused on solar-PV power system modeling. Several studies already address that [7] [8] [9]. However, the control mechanism for an inverter-based scheme with a DC-DC converter is modeled and analyzed. Similarly, the control implementation of a grid-supporting system for a solar-photovoltaic system is used with the droop, and a DC-DC converter was developed. Modeling and emulating this system through simulation are critical to investigating how the inverter-based microgrid responds to FRT/LVRT technical challenges, among other issues. This is valuable for

our analysis, design, and verification; hence, the inverter-based microgrid with a DC-DC power converter discrete-time model was developed.

FRT is one of the critical technical issues in large-scale PV grid integration with a less thorough study. A methodology to limit the active power generated by the MPPT is introduced for an inverter-based microgrid with a DC-DC converter. A unique control scheme is implemented to curtail the DC power produced and equip the interfacing power converters with fault ride-through qualities, to minimize the prospect of triggering the overvoltage protection scheme of the DC link. This is achieved without shutting down the voltage-boosting operation of the converter. The DC bus voltage of the DC-DC and DC-AC converters is controlled during the AC grid voltage sag cycle. Consequently, the solutions proposed in this study curtailed the usual momentous DC voltage increase in the DC bus under transient conditions.

2. DC-DC Conversion Phase and MPPT Control

In integrating solar PV systems with the AC grid, the DC-DC conversion phase is critical in ensuring optimal power extraction. This phase incorporates MPPT control, which continuously adjusts the operating point of the PV panels to maintain operation at the MPP. By tracking and adapting to changing environmental conditions, such as solar irradiance and temperature variations, the MPPT control enables the PV system to harvest the maximum available power from the solar resource. On the other hand, the DC-AC inverter phase is responsible for efficiently converting the DC power output of the PV system into AC power compatible with the AC grid. This conversion process involves adjusting the voltage magnitude and frequency of the solar PV source to match the AC grid requirements. The inherent intermittencies in solar PV generation, caused by factors like cloud cover or shading, can result in mismatches between the PV source current and voltage and the AC grid voltage magnitude and frequency. Power electronic-based interfaces, such as the DC-AC inverter, are indispensable in addressing this issue [10].

These power electronic interfaces provide essential functions to ensure reliable, secure, and efficient energy conversion from solar PV systems. They facilitate the transformation of DC power from the PV panels to AC power suitable for grid integration. Additionally, power electronic converters enable grid synchronization and control, ensuring that the PV system operates in harmony with the AC grid. The power electronic converters ensure a smooth and stable power transfer from the PV system to the grid by controlling the voltage and frequency outputs. The integration of power electronic-based interfaces into solar PV systems brings several advantages. Firstly, it enhances the reliability and security of energy conversion. Power electronic converters allow advanced protection mechanisms, such as fault detection and isolation, to safeguard the system against potential failures or disturbances. Moreover, the modular nature of power electronic systems enables the PV system to continue operating even if a specific component or section experiences an issue, improving overall system reliability.

Furthermore, power electronic converters contribute to higher energy conversion efficiency. These devices employ advanced switching techniques and control algorithms that minimize power losses during conversion. By efficiently matching the PV system's output characteristics to the AC grid requirements, power electronic interfaces maximize the energy yield and minimize wasted energy, improving overall system efficiency. Power electronic converters' design, operation, and control should be carefully considered despite their numerous benefits. Adequate design considerations include selecting appropriate converter topologies, sizing the components correctly, and ensuring thermal management to handle the power levels involved. Proper operation and control strategies must be implemented to optimize system performance, maintain stability, and meet grid code requirements. Thus, integrating power electronic-based interfaces, including MPPT control in the DC-DC conversion phase and efficient power delivery through DC-AC inverters, is essential for reliable and efficient energy conversion from solar PV systems to the AC grid. These interfaces address the mismatch between PV source characteristics and grid requirements, enabling more secure and efficient power transfer. However, careful attention should be given to the design, operation, and control of power electronic converters to ensure optimal performance and successful integration of solar PV systems with the AC grid [11].

The rating of the DC-DC converter used in a solar PV system strongly relies on two main factors: the PV modules' probable voltage range and the DC-AC inverter's required input voltage. A relatively high DC link voltage, reaching up to 1000V, is necessary for a grid-connected DC-AC inverter system. The DC-DC converter plays a crucial role in adjusting the voltage levels to meet these requirements. The DC-DC converter operates in boost mode to step up the nominal voltage when it is lower than the required reference for the inverter. Conversely, when the voltage exceeds the required inverter voltage, the buck mode is activated to limit the voltage. Figure 1 illustrates the operation of the DC-DC converter in boost mode. It consists of an IGBT (Insulated-Gate Bipolar Transistor) block denoted as G, a semiconductor device controlled by the gate signal. The figure shows that an inductor (L) and a semiconductor diode (S) are connected to the IGBT block. Additionally, two capacitors, C_{PV} and C_{DC}, are connected to the input and output of the DC-DC boost converter, respectively.

In this configuration, during the boost mode operation, the IGBT block is controlled to switch on and off at specific intervals. When the IGBT is switched on, the current flows through L and charges up the C_{PV} capacitor, increasing the voltage. At the same time, S blocks the reverse current flow. When the IGBT is switched off, the inductor discharges its stored energy into the output capacitor (C_{DC}), effectively stepping up the voltage. The boost mode operation of the DC-DC converter enables the adjustment of the PV module voltage to match the requirements of the DC-AC inverter. By increasing the voltage when needed, the converter ensures

that the DC link voltage reaches the desired level for proper grid integration.

The C_{PV} and C_{DC} capacitors play essential roles in the DC-DC converter. C_{PV}, connected to the converter's input, helps in smoothing out the input voltage and provides a stable source for the boost operation. On the other hand, CDC is connected to the converter's output and acts as a buffer to store energy and supply a constant voltage to the DC-AC inverter. Careful consideration of the DC-DC converter's design and selection of its components, such as the IGBT, inductor, diode, and capacitors, is crucial to ensure reliable and efficient operation. Proper sizing of these components and thermal management considerations is essential to handle the power levels involved and ensure the converter's performance and longevity. Thus, the rating of the DC-DC converter used in a solar PV system depends on the PV modules' probable voltage range and the DC-AC inverter's input voltage requirements. The converter operates in boost mode to step up the voltage when needed and employs components such as the IGBT, inductor, diode, and capacitors to facilitate the voltage conversion. The DC-DC converter enables efficient and reliable power transfer from the PV system to the AC grid through careful design and component selection.

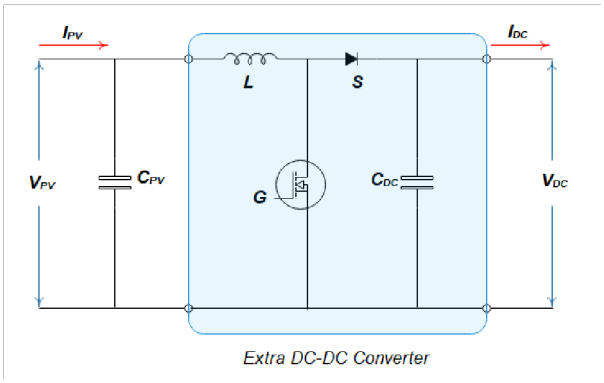

Fig. 1. DC-DC converter schematic controlling.

$$V_{dc} = \frac{1}{1-d} V_{PV} \tag{1}$$

In the operation of the boost converter depicted in Figure 1, a pulse-width modulation (PWM) signal is utilized to control the switching of the IGBT block. This PWM signal alternates between "on" and "off" states over a specific period. The duty cycle (denoted as 'd') of the PWM signal determines the voltage ratio between the input voltage (VPV) from the solar PV source and the output voltage (Vdc) of the DC link. Equation 1 represents this relationship [12]. The individual circuit components shown in Figure 1 are combined to create a model that can be used for simulation and analysis of the boost converter. The IGBT block is controlled by the preferred duty cycle, which is determined based on system requirements and operating conditions. A large capacitor is typically employed in simulation to maintain a steady output voltage.

MPPT (maximum power point tracking) control algorithms are essential to achieve maximum power extraction from the solar PV system. These algorithms consider the intermittent nature of PV generation caused by factors such as solar irradiance, temperature variations, and shading. Numerous MPPT control algorithms have been developed and implemented to achieve optimum system performance. The MPPT control algorithm senses the PV modules' current and voltage to evaluate the boost converter's duty ratio ('d'). By adjusting the duty cycle, the MPPT control algorithm ensures that the converter operates at the PV system's maximum power point (MPP), where the output power is maximized. The duty cycle information is then used to generate the appropriate PWM signal for the gate driver, which controls the IGBT switching.

Through the coordinated operation of the MPPT control algorithm, the PWM signal controller, and the IGBT, the boost converter maintains efficient power conversion by continuously adapting to changes in PV module characteristics and environmental conditions. This dynamic control enables the system to harvest the maximum available power from the PV modules and enhance overall system performance. The design and selection of MPPT control algorithms and the PWM signal controller and gate driver are important considerations for achieving accurate and responsive control of the boost converter. The entire system's performance and reliability depend on these control components' effectiveness.

Thus, the boost converter's operation is controlled by a PWM signal, with the duty cycle determining the voltage ratio between the input voltage from the solar PV source and the output voltage of the DC link. Considering the intermittent nature of PV generation, MPPT control algorithms are crucial for maximum power extraction. These algorithms evaluate the duty ratio based on PV module current and voltage measurements, and the resulting PWM signal controls the IGBT switching through the gate driver. Effective control strategies and components ensure optimal system performance and efficient power conversion from the solar PV system.

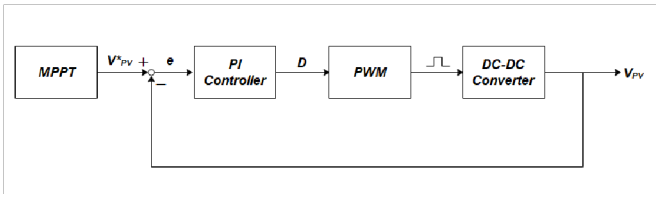

Fig. 2. Feedback loop model PV voltage control.

$$I_{PV} V_{PV} = v_d i_d + v_q i_q \tag{2}$$

$$i_d^{\approx} = \frac{I_{PV} V_{PV}}{v_d} \tag{3}$$

In this work, the extremum-seeking maximum power point tracking (MPPT) technique known as incremental conductance (IC) was implemented. The IC technique is a well-established method that aims to match incremental conductance with the instantaneous conductance of the photovoltaic (PV) system. The IC algorithm drives the PV system towards the maximum power point (MPP) by continuously adjusting the voltage based on the comparison

results. Unlike the perturb and observe (P&O) procedure, where the voltage is perturbed, and the resulting power is observed, the IC algorithm eliminates the continuous perturbation once the MPP is reached. Instead, it relies on observing and interpreting the slope of the power-voltage (P-V) curve to regulate the modelled DC-DC converter and maintain operation at the MPP.

The IC algorithm is based on the observation and interpretation of the slope of the P-V curve. At the MPP, the slope is zero (dPPV/dVPV = 0), indicating that the power (PPV) is maximized with respect to the voltage (VPV). On the left side of the MPP, the slope is positive (dPPV/dVPV = +ve), while on the right side, it is negative (dPPV/dVPV = -ve). These slope characteristics serve as key indicators for the IC algorithm to adjust the voltage and seek the MPP. The IC algorithm continuously monitors the slope of the P-V curve and adjusts the voltage accordingly to maintain or approach the zero slope condition. If the slope is positive, indicating that the system is on the left side of the MPP, the algorithm reduces the voltage to approach the MPP. Conversely, if the slope is negative, indicating that the system is on the right side of the MPP, the algorithm increases the voltage to drive toward the MPP.

It is important to note that the IC algorithm operates based on the principle that instantaneous conductance can be estimated by observing the variations in power and voltage. By closely monitoring the slope and employing appropriate control actions, the algorithm ensures that the PV system operates as close as possible to the MPP. Implementing the IC algorithm in this work involves integrating it with the modelled DC-DC converter. The IC algorithm adjusts the converter's control parameters to enable efficient and accurate tracking of the MPP. By dynamically regulating the voltage, the IC algorithm allows the PV system to adapt continuously to changing environmental conditions and maintain operation at the MPP, thereby maximizing power extraction.

Thus, this work utilized the incremental conductance (IC) algorithm as an extremum-seeking MPPT technique. The IC algorithm matches incremental conductance with instantaneous conductance and adjusts the voltage to approach the maximum power point (MPP). The algorithm operates based on observing and interpreting the slope of the power-voltage curve, aiming for a zero slope at the MPP. By integrating the IC algorithm with the DC-DC converter, the system achieves accurate MPP tracking and enhances the overall performance of the PV system.

The boost converter utilizes an inner control loop to regulate the converter to a specified reference, with the MPPT algorithms responsible for setting this reference. This control loop ensures that the converter's input voltage matches the desired output voltage. Figure 2 illustrates the configuration of the boost converter, and Equation 2 expresses the VPV input voltage. In order to achieve the desired input PV voltage, feedback control is implemented. The feedback loop model, as shown in Figure 2, involves sampling the converter voltage and feeding it back to the controller through a summing block to extract the error. The controller then generates the appropriate duty cycle, attenuating the error and adjusting the input voltage to maintain it at the specified reference.

The feedback loop operates as follows: the input PV voltage (VPV) is compared to the reference voltage within the summing block. The resulting error, which represents the difference between the actual input voltage and the desired reference, is then passed to the controller. The controller processes the error and generates a corresponding duty cycle that will bring the input voltage closer to the reference. By adjusting the duty cycle, the controller effectively regulates the converter's operation, ensuring that the input voltage matches the desired reference voltage [13]. This feedback control loop enables the system to respond to changes in operating conditions and maintain the desired voltage output.

It is important to note that the configuration of the boost converter and the feedback control loop can vary depending on the specific implementation and control strategy. Different control techniques and algorithms can be employed to achieve optimal performance and accurate converter regulation. Consequently, the boost converter incorporates an inner control loop to regulate the converter to a specified reference, with the MPPT algorithms determining this reference. As illustrated in Figure 2, the feedback control loop utilizes a summing block to extract the error by comparing the input PV voltage to the reference voltage. The controller processes this error and generates a duty cycle that adjusts the input voltage to match the desired reference. This feedback control mechanism ensures that the converter operates at the desired voltage output, enhancing the overall performance and efficiency of the system [14].

In inverter-based microgrids where a DC-DC power converter is used for grid integration of solar photovoltaic (PV) systems, the VPV (PV voltage) is regulated through the control of the duty ratio. To improve the dynamics of the DC bus voltage, a feed-forward scheme is employed, assuming there is no conversion loss from DC to AC power. This implies that the power on the DC side of the PV system is equivalent to the power transmitted to the AC grid on the AC side, as expressed in Equation 3. In this equation, P_DC represents the power on the system's DC side (PV side), while P_AC represents the power on the AC side (grid side). By ensuring that the DC power is equal to the AC power, the feed-forward scheme aims to maintain efficient power transfer and minimize losses.

In addition, the quadrature-axis component voltage (Vq) is forced to zero value by the proportional-integral (PI) controller of the phase-locked loop (PLL). The PLL synchronizes the inverter with the grid and maintains a constant frequency and phase relationship. By setting Vq to zero, the focus is primarily on controlling the direct-axis component of the current. With this setup, the estimated direct-axis current component, which is a function of the PV variable, can be obtained using Equation 3 [15]. This equation allows for the estimation of the direct-axis current component based on the PV system's operating conditions and characteristics.

It is important to note that the specific implementation of the feed-forward scheme and the equations and control

strategies used may vary depending on the system requirements and design. This approach aims to optimize the grid integration of the solar PV system, enhance the power transfer dynamics, and maintain a stable and reliable operation of the microgrid. Thus, for inverter-based microgrids utilizing a DC-DC power converter for solar PV grid integration, the VPV is regulated through the control of the duty ratio. A feed-forward scheme is implemented to improve the dynamics of the DC bus voltage by assuming no conversion losses from DC to AC power. This scheme ensures that the power on the DC side is equivalent to the power transmitted to the AC grid. The PLL's PI controller sets the quadrature-axis component voltage to zero, allowing for the estimation of the direct-axis current component based on the PV system's characteristics. The overall aim is to achieve efficient and reliable grid integration of the solar PV system within the microgrid.

3. DC-AC Inverter and Modified Grid-Supporting

In inverter-based microgrids employing a boost converter, the grid-tied inverter plays a crucial role in synchronizing with the AC grid frequency and delivering the available power generated by the solar PV system to the electric power network. The purpose of the grid-tied inverter is to convert the DC power from the PV system into AC power that can be seamlessly integrated with the AC grid. To ensure proper operation, the voltage of the DC link, which connects the boost converter to the inverter, needs to be maintained at a level higher than the magnitude of the grid voltage. This voltage requirement ensures that the inverter can effectively transfer power to the AC network and maintain a stable connection.

The inverter controller is a key component that enables the efficient delivery of DC power from the PV system to the AC network and provides high-level functionality for grid interaction. One of the primary functions of the inverter controller is to synchronize the AC grid voltage with the output of the inverter. This synchronization is achieved through the use of a phase-locked loop (PLL), which detects the frequency and phase of the AC grid voltage and adjusts the inverter's output accordingly [16]. The primary control of the inverter controller calculates and supplies a corresponding duty cycle to the pulse width modulator (PWM). The duty cycle determines the duration of time during each switching cycle that the inverter's IGBT-Diode switches are turned on or off. The PWM generates the necessary control signals for the IGBT-Diode switches, enabling them to produce appropriate output waveforms that match the desired AC grid voltage and frequency.

By effectively controlling the duty cycle and switch operation, the inverter controller ensures that the power delivered from the PV system is synchronized with the AC grid, maintaining a stable and reliable connection. This control mechanism enables the grid-tied inverter to deliver the maximum available power from the PV system to the electric power network while complying with grid requirements and regulations. Thus, in inverter-based microgrids utilizing a boost converter, the grid-tied inverter is responsible for synchronizing with the AC grid frequency and delivering the power generated by the solar PV system to the electric power network. With its PLL and primary control, the inverter controller ensures synchronization, regulates the duty cycle, and operates the IGBT-Diode switches to produce appropriate output waveforms. This enables efficient power transfer from the PV system to the AC grid and facilitates high-level grid interaction functionality.

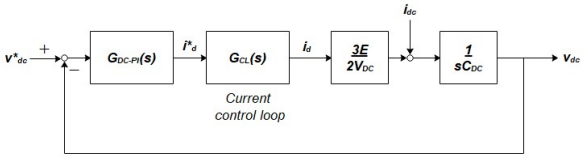

Fig. 3. DC-link bus voltage loop applying power balance equation.

Several fundamental control requirements must be addressed in grid-connected inverter-based microgrids utilizing a DC-DC interface power converter to ensure efficient and high-quality operation. These requirements include maximum power point tracking (MPPT) for optimal power extraction, high-quality power injection with low total harmonic distortion (THD) in voltage and current waveforms [17]. To fulfill these demands, the primary controller is typically divided into two cascading control loops: an outer loop for power or voltage control and an inner loop for current control. The outer loop, as shown in Figure 3, generates the reference current that the inner control loop will use. The objective of the outer loop is to regulate the power or voltage at the point of the grid connection. By accurately tracking the solar PV system's maximum power point (MPP), the MPPT algorithm determines the reference current required for maximum power extraction from the PV panels. This reference current is then passed on to the inner control loop for further regulation.

The inner loop, known as the current control loop, plays a crucial role in regulating the currents and, consequently, the power injected into the grid. Its primary function is to ensure that the currents flowing through the inverter and injected into the grid are precisely controlled and meet the required quality standards. By maintaining accurate and stable current control, the inner loop helps to minimize harmonic distortions and maintain the desired power quality. By combining the outer power or voltage control loop and the inner current control loop, the primary controller in the microgrid ensures effective power injection into the grid while meeting the specific control objectives. The cascading control structure enables precise power flow regulation and maintains the desired voltage and current waveforms within the grid-connected system.

It is worth noting that the control strategies and algorithms employed in the outer and inner loops can vary depending on the specific microgrid requirements and system design. Various control techniques, such as proportional-integral (PI) control or model predictive control (MPC), can be utilized to achieve accurate and efficient control performance. Thus, grid-connected inverter-based microgrids with a DC-DC interface power converter need to fulfill

essential control demands such as MPPT and high-quality power injection with low THD voltage and current waveforms. The primary controller is typically divided into two cascading control loops: an outer loop for power or voltage control and an inner loop for current control. The outer loop generates the reference current based on MPPT algorithms, while the inner loop regulates the currents and ensures accurate and high-quality power injection into the grid. Combining these control loops allows the microgrid to achieve efficient and reliable operation while adhering to the specific control objectives.

3.1. Outer Control Loop

In an inverter system with a DC-DC power converter, a capacitor with a significant capacity is installed at the DC-link to ensure the balance of power between the DC and AC sides. This capacitor plays a crucial role in regulating and smoothing the DC input power before it is transmitted into the AC side through the inverter. Its purpose is to maintain a stable and controlled DC-link voltage, directly affecting the amount of power injected into the AC grid. The DC-link voltage regulation is essential for controlling the active power injected into the AC grid. As depicted in Figure 3, the DC-link voltage is controlled to regulate the power flow. The outer loop control of the system ensures that the DC-link voltage remains constant, thereby maintaining the PV source's grid connection. However, it is important to note that the magnitude of the DC-link voltage is relatively higher than the magnitude of the AC grid voltage to ensure the appropriate power injection into the AC side.

The power at the DC side can be expressed using Equation 4, which considers the DC-link voltage and the current flowing through the DC side. Similarly, the active power injected into the AC grid is given by Equation 5. The power balance principle dictates that the input power on the DC side should be equal to the output power on the AC side, assuming negligible power losses in the DC-AC inverter.

A PI (proportional-integral) controller is typically implemented to regulate the voltage at the DC link. The PI controller generates a corresponding direct-axis reference current, as shown in Equation 6, to achieve the desired DC-link voltage. This reference current aligns the direct-axis voltage component (Vd) with the AC grid voltage, ensuring the power balance between the DC and AC sides. The transfer function representing the DC-link voltage plant is derived, enabling small-signal analysis and system linearization. Therefore, the capacitor installed at the DC-link in an inverter system with a DC-DC power converter balances and regulates the power between the DC and AC sides. By controlling the DC-link voltage, the capacitor ensures that the injected power into the AC grid remains stable and within desired limits. The PI controller regulates the voltage at the DC-link, generating the appropriate direct-axis reference current. This control mechanism enables efficient power transfer and maintains the power balance between the DC and AC sides of the system.:

$$P_{dc} = v_{dc} i_{dc} - v_{dc} C_{dc} \frac{dv_{dc}}{dt} \tag{4}$$

$$P_{ac} = \frac{3}{2}\left(v_d i_d + v_q i_q\right) \tag{5}$$

$$v_{dc}(s) = i_d(s) G_{dc}(s) = i_d(s) \frac{3E}{2\left[I_{dc} - sC_{dc}V_{dc}\right]} \tag{6}$$

To achieve precise control of the DC-link voltage and current in the inverter system with a DC-DC power converter, PI (proportional-integral) controllers are commonly employed. These controllers are crucial in regulating the system's behavior and maintaining the desired operating conditions. The PI controller for the DC-link voltage control is applied to the transfer function of the DC-link voltage plant, denoted as GDC(s). The controller parameters include kp-dc (proportional gain), ki-dc (integral gain), and Ti-dc (integral gain time constant). The proportional gain determines the immediate response of the controller to deviations in the DC-link voltage, while the integral gain accounts for the accumulated error over time. The integral gain time constant, Ti-dc, determines the rate at which the integral term responds to the error.

Similarly, the current control loop is designed using a PI controller. The current control loop aims to regulate the currents flowing through the inverter and ensures accurate and precise power injection into the AC grid. The PI controller parameters for the current control loop are kp-cl (proportional gain), ki-cl (integral gain), and Ti-cl (integral gain time constant). These parameters determine how the controller responds to deviations in the current and how it accumulates and adjusts for the error over time. By incorporating these PI controllers into the system, the overall control of the DC voltage open-loop is modeled. The PI controllers continuously monitor and adjust the system's behavior to maintain the desired DC-link voltage and current levels. Through proportional and integral control actions, the controllers effectively regulate the plant transfer functions and provide the necessary control signals to achieve stable and accurate control performance.

It is important to note that the specific values for the proportional and integral gains and the time constants are typically determined through system analysis, simulation, and tuning processes. The selection of these parameters depends on the system requirements, performance objectives, and stability considerations. Proper tuning of the PI controllers is crucial to ensure optimal and robust control performance in the inverter system with a DC-DC power converter.

3.2. Inner Current Loop Control

In the control system of the inverter-based microgrid with a DC-DC power converter, the direct-axis (d-axis) and quadrature-axis (q-axis) components are interrelated, which introduces some complexities in their independent control. Additionally, the AC grid voltage influences the control

system's dynamics. To address these challenges, improvements can be made to the dq references of the output voltage by incorporating feed-forward dq voltage and decoupling components. By subtracting the feed-forward dq voltage from the references, the control system achieves better accuracy and performance in regulating the output voltage.

Furthermore, the dq output currents that are injected into the grid can be decoupled to align with the desired modulation signal. This decoupling ensures that the control system operates efficiently and independently for each axis, reducing the influence of one axis on the other. To analyze and model the system's behavior in the frequency domain, the Laplace Transform is applied to derive the s-domain equivalent representation. This transformation allows for a comprehensive understanding of the system dynamics and enables the design of appropriate control strategies in the frequency domain.

By considering the interdependence of the d-axis and q-axis components, incorporating feed-forward techniques, and decoupling the output currents, the control system can achieve improved performance and enhanced regulation of the inverter-based microgrid. These measures help mitigate the complexities arising from the interrelationships between the components and the influence of the AC grid voltage, resulting in more precise control and reliable operation.

3.3. Grid Supporting Control

In the overall control scheme of an inverter-based microgrid with a DC-DC power converter, achieving control over grid frequency and voltage regulation is a crucial objective. Figure 7 illustrates the layout of the entire system and demonstrates how this objective can be accomplished by implementing concurrent active power and reactive power control using droop control techniques. In the case of a solar-photovoltaic system, the active power output of the inverter is determined using Pω droop control. This control scheme emulates the inertial response exhibited by synchronous generators. The Pω droop control adjusts the active power output of the inverter based on the deviation between the actual grid frequency (ω) and the reference frequency. By incorporating this droop control, the inverter actively contributes to regulating the grid frequency, maintaining it within the desired range [18].

Additionally, the reactive power output of the voltage-source inverter is determined using Q-E droop control. The Q-E droop control adjusts the reactive power output based on the deviation between the actual grid voltage magnitude (E) and the reference voltage. This control scheme ensures that the inverter actively regulates the grid voltage, enabling effective voltage support and stability. By implementing concurrent active power and reactive power control using droop control techniques, the overall control scheme of the inverter-based microgrid with a DC-DC power converter can effectively regulate both the grid frequency and voltage. This control strategy enables the system to mimic the behavior of synchronous generators and contribute to grid stability and reliability. The specific parameters and characteristics of the droop control, such as the droop coefficients, need to be carefully determined and tuned based on the system requirements and operational conditions. Proper tuning ensures optimal performance and coordination between the different control objectives, allowing the system to respond accurately and efficiently to variations in grid conditions.

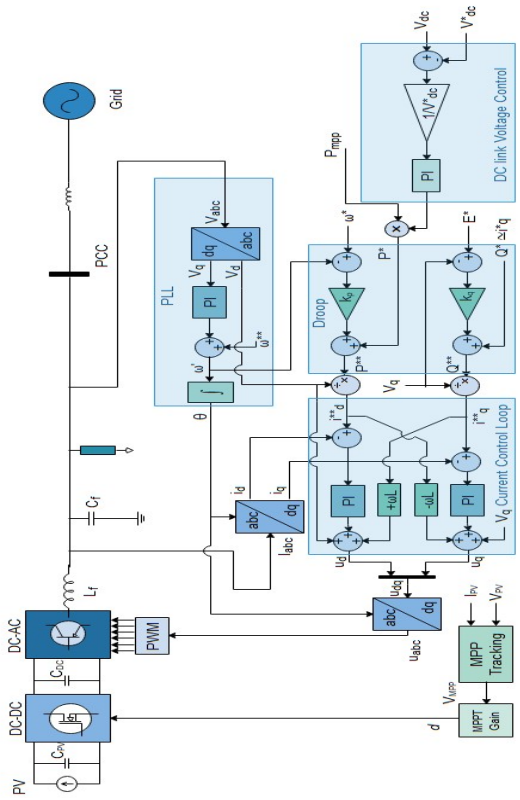

Fig. 4. Grid Supporting Control with Droop for Inverter-based.

Microgrid with a DC-DC Converter for Solar-PV integration

3.4. Delayed Signal Cancellation

In order to ensure that the microgrid and main grid system voltage remain within the specified limits set by the grid code (such as the maximum allowable voltage) and the required voltage range (typically 90-110% of the nominal voltage), voltage control mechanisms are implemented. To address unbalanced grid voltage conditions, the symmetrical component equivalent is extracted. This involves decomposing the grid voltage into positive, negative, and zero sequence components. By identifying these symmetrical components, appropriate unbalanced compensation techniques can be applied to regulate the grid voltage.

In Part 2 of the system implementation, a Digital Signal Controller (DSC) interface is utilized to identify the symmetrical components of the grid voltage. The DSC interface employs algorithms and calculations to analyze the grid voltage waveform and extract the positive, negative, and zero sequence components. Each component is evaluated separately to determine its respective values. To ensure accurate analysis and response to grid variations, a time of 5ms is chosen as the sampling time for a grid frequency of

50 Hz. This sampling time is calculated using the formula: Nd = fs / (4f1), where fs is the sampling frequency and f1 is the fundamental frequency of 50 Hz, representing the grid frequency in this specific study example.

By accurately identifying and evaluating the symmetrical components of the grid voltage using the DSC interface, appropriate control strategies can be implemented to compensate for unbalanced voltage conditions. This enables the microgrid and main grid system to maintain voltage levels within the prescribed limits, ensuring compliance with grid code requirements and safeguarding the stability and reliability of the overall electrical power system.

The DSC algorithm relies on evaluating the three-phase voltage and its subsequent decomposition into equivalent symmetrical components [19]. In the stationary reference frame, the voltages measured in the three phases can be represented using the Clarke (abc-αβ) transformation, as given by Equation 7. In this equation, [a b c]T represents the vector of three-phase voltages, and [α β γ]T represents the vector of transformed voltages in the stationary reference frame. The transformation is performed using a scaling factor of √(2/3) to maintain the magnitude of the transformed voltages.

The Clarke transformation enables the conversion of three-phase voltages from the abc (phase) reference frame to the αβ reference frame. The resulting αβ components represent the positive and negative sequence components of the three-phase voltage, which are essential for analyzing and controlling the voltage asymmetry in the system. By applying the Clarke transformation, the DSC algorithm can accurately evaluate the symmetrical components of the voltage, allowing for effective analysis and control strategies to address voltage imbalances and ensure proper voltage regulation within the microgrid and main grid system.

The DSC algorithm involves additional steps beyond the Clarke transformation to extract and evaluate the symmetrical components. These steps may include further calculations, such as Park transformation, to obtain the positive, negative, and zero sequence components. The DSC algorithm combines these components to assess the voltage quality and implement appropriate control measures for maintaining stable and balanced operation within the electrical power system.

$$\begin{bmatrix} v_\alpha \\ v_\beta \end{bmatrix} = \begin{bmatrix} 1 & 0 & 0 \\ 0 & \frac{\sqrt{3}}{3} & -\frac{\sqrt{3}}{3} \end{bmatrix} \cdot \begin{bmatrix} v_a \\ v_b \\ v_c \end{bmatrix} \quad (7)$$

In conjunction with the stationary reference frame obtained in Equation 8, two opposite sequence rotations are implemented using the calculated phase angle of the AC grid voltage (θ and -θ). The angle θ is the same as the angle θ obtained from the output of the phase-locked loop (PLL). Equation 8 represents the positive sequence component, while Equation 9 represents the negative sequence component [20] [21]. In these equations, [α β]T represents the transformed voltage components in the stationary reference frame obtained through the Clarke transformation. The complex exponential term exp(jθ) performs a positive sequence rotation, while exp(-jθ) represents a negative sequence rotation. By applying these sequence rotations, the positive sequence components [αs βs]T and negative sequence components [αn βn]T can be determined.

The positive sequence components [αs βs]T correspond to the symmetrical components of the voltage waveform that contribute to the positive sequence, while the negative sequence components [αn βn]T represent the symmetrical components associated with the negative sequence. These sequence rotations are integral to the DSC algorithm as they allow for the separation and analysis of the voltage's positive and negative sequence components. By evaluating these components, the algorithm can detect and address any imbalances or deviations from the desired voltage profile, facilitating effective microgrid and main grid system control.

The phase angle θ used in the sequence rotations is typically obtained from the output of the phase-locked loop (PLL). The PLL ensures synchronization of the inverter output with the AC grid voltage, providing the necessary reference for the sequence rotations and enabling accurate assessment of the positive and negative sequence components. By utilizing Equations 8 and 9 in conjunction with the calculated phase angle, the DSC algorithm can effectively extract and evaluate the positive and negative sequence components, enabling comprehensive analysis and control of the system's voltage characteristics.

The estimated values for vqp (positive sequence component) and vqn (negative sequence component) are stored in two separate data buffers for a duration equal to half a cycle, representing a half-life period. The purpose of these buffers is to collect and retain the final samples of the positive and negative components within this duration. Equations 10 to 13 outline the specific components and their additions involved in this process.For the positive sequence component, Equations 10 and 11 are used. In these equations, vqp(i) represents the estimated positive sequence component at the current time step (i), while vqp(i-1) represents the previous estimated value. The term vqp_new represents the newly calculated value for the positive sequence component based on the current input samples. The coefficient α determines the weighting between the previous and new values, allowing for gradual updates and smoothing of the estimated component.

Similarly, for the negative sequence component, Equations 12 and 13 are used: In these equations, vqn(i) represents the estimated negative sequence component at the current time step (i), while vqn(i-1) represents the previous estimated value. The term vqn_new represents the newly calculated value for the negative sequence component based on the current input samples. Similar to the positive sequence component, the coefficient α determines the weighting between the previous and new values.

The second term samples in Equations 10 to 13 refer to the components of the first term but shifted by a duration of one-fourth of a cycle. This shift is expressed as a multiple of the second term, indicating a time delay in the calculations.

By employing these equations and the corresponding buffering scheme, the DSC algorithm can effectively estimate and update the positive and negative sequence components of the voltage waveform. This information is crucial for assessing and compensating for any imbalances or asymmetries in the grid voltage, allowing for improved control and regulation of the microgrid and main grid system.

The DSC algorithm proposed in this work is visually depicted in Figure 5. In Figure 5(a), two components, t1 and t2, of vdp(k), vqp(k), vdn(k), and vqn(k) are rotated counter-clockwise. This rotation is represented by the arrows indicating the direction of the rotation. Subsequently, in Figure 5(b), a fundamental delay cycle is applied to the components vdp(k), vqp(k), vdn(k), and vqn(k). This delay cycle is equal to k minus fs/(4.fg), where fs is the sampling frequency and fg is the fundamental frequency of the grid. This delay introduces a phase shift delay of -π to the component t1 and a phase shift delay of -2π to the component t2.

To compensate for the phase shift introduced in Figure 5(b), a backward rotation clock responds by adding a phase shift of +π to the two components' phases. This brings t1 back to its initial position and reduces t2 to zero. As a result of these rotations and compensations, t1 is doubled in length, while t2 is eliminated. By superimposing Figures 5(a) and 5(b), the resulting waveform is shown in Figure 5(c). This waveform represents the outcome of the DSC algorithm, where the desired symmetrical components have been extracted and the phase shifts have been compensated for. The waveform in Figure 5(c) reflects the improved estimation and separation of the symmetrical components, which is essential for subsequent analysis and control in the overall system.

During grid failure, the voltage sequence components at the Point of Common Coupling (PCC) can be obtained in the d-q coordinates using Equations 10 to 13. The PCC-independent voltage control systems are then employed to restore the standard sequence references. The positive sequence control aims to bring the positive sequence level of the PCC voltage back to its rated value. By regulating the positive sequence component, the voltage at the PCC can be restored to its desired level, mitigating any deviation caused by the grid failure.

Similarly, the negative sequence regulation focuses on restoring the quadrature component of the PCC voltage to a zero standard condition. This means that the negative sequence control ensures that the quadrature component, which represents the unbalanced portion of the voltage, is reduced to zero. By controlling both the positive and negative sequence components of the PCC voltage, the unbalance in voltage created by injecting reactive power into the grid can be effectively checked and buffered. This helps in maintaining the stability and quality of the voltage at the PCC, even during grid disturbances or failures.

$$\begin{bmatrix} v_\alpha^p \\ v_\beta^p \end{bmatrix} = \begin{bmatrix} \cos\theta & \sin\theta \\ -\sin\theta & \cos\theta \end{bmatrix} \cdot \begin{bmatrix} v_\alpha \\ v_\beta \end{bmatrix} \tag{8}$$

The negative component implies

$$\begin{bmatrix} v_\alpha^n \\ v_\beta^n \end{bmatrix} = \begin{bmatrix} \cos\theta & -\sin\theta \\ \sin\theta & \cos\theta \end{bmatrix} \cdot \begin{bmatrix} v_\alpha \\ v_\beta \end{bmatrix} \tag{9}$$

$$v_{\alpha\beta}^p = \frac{1}{2}\left[v_{\alpha\beta}(t) - jv_{\alpha\beta}\left(t - \frac{f_s}{4 \cdot f_g} \right) \right] \tag{10}$$

$$v_{\alpha\beta}^n = \frac{1}{2}\left[v_{\alpha\beta}(t) + jv_{\alpha\beta}\left(t - \frac{f_s}{4 \cdot f_g} \right) \right] \tag{11}$$

$$v_{\alpha\beta}^p = \frac{v}{\left[1 - e^{-j2\theta_d}\right]} = \frac{1}{2}\left[\frac{\left[v_{\alpha\beta}(\omega t) - e^{-j\theta_d} v_{\alpha\beta}(\omega t - \theta_d) \right]\left(1 - e^{j2\theta_d}\right)}{1 - \cos(2\theta_d)} \right] \tag{12}$$

$$v_{\alpha\beta}^n = \frac{1}{2}\left[\frac{\left[v_{\alpha\beta}(\omega t) - e^{j\theta_d} v_{\alpha\beta}(\omega t - \theta_d) \right]\left(1 - e^{-j2\theta_d}\right)}{1 - \cos(2\theta_d)} \right] \tag{13}$$

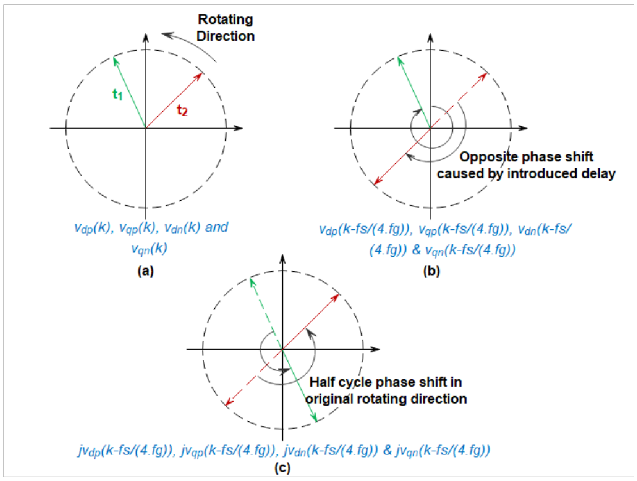

Fig. 5. Delayed Signal Cancellation Demonstration.

4. Results and Discussions

The grid in the system operates at a phase-to-phase RMS voltage of 11 kV. A step-up transformer with a voltage ratio of 400/11000 V is installed to interface the microgrid with the grid. This transformer converts the voltage from the microgrid to the grid voltage level, allowing proper integration of the DC power generated by the microgrid into the AC grid. The DC-AC inverter control system is crucial in efficiently delivering the extracted DC power to the AC grid. The control system employs a two-loop current control strategy. The outer loop, the power loop, controls the DC-link voltage. This loop generates the dq references for the current used by the internal current control loop, as shown in Figure 8. The purpose of the power loop is to regulate the DC-link voltage at the desired level, ensuring stable operation of the inverter.

On the other hand, the inner loop generates the reference dq voltage that serves as the input for the pulse width modulation (PWM) control of the inverter. This inner loop regulates the inverter's output voltage, ensuring that it follows the desired waveform and meets the requirements of the AC grid. By employing these two current control loops, the DC-AC inverter effectively manages the power flow between the microgrid and the AC grid, ensuring efficient and reliable operation of the system [22].

The voltage of the photovoltaic (PV) system, VPV, is controlled by adjusting the duty cycle, denoted as d, of the power converter. The duty cycle represents the ratio of time during which the power converter is "on" compared to the total switching period. The power converter can regulate the voltage output by varying the duty cycle. To achieve maximum power point tracking (MPPT), a controller is employed to determine the optimal duty cycle for the given PV conditions. The MPPT controller continuously monitors the PV system's voltage and current, and based on this information, it calculates the appropriate duty cycle that maximizes the power output of the PV system.

The calculated duty cycle from the MPPT controller is then supplied as the pulse width modulation (PWM) input to the DC-DC converter. The controller generates the PWM signals to control the switching of the DC-DC converter's switches. These switches are operated according to the PWM signals, allowing the converter to produce the desired output waveforms. The PV system can effectively regulate its voltage and optimize power extraction from the solar panels by adjusting the duty cycle through the MPPT controller and controlling the DC-DC converter's switches with PWM signals. This enables efficient operation and maximum power generation from the PV system.

In Figure 9, the DC link voltage, denoted as VDC, exhibits a relatively stable fluctuation within a certain range. At steady-state operation, around 0.5 seconds, VDC becomes relatively constant at 1000 V. This constant voltage is maintained with respect to the PWM switching frequency of 5000 Hz, which corresponds to a period of 0.0002 seconds. The duty cycle, denoted as d, is precisely adjusted to regulate the input voltage VPV from the PV arrays. By fine-tuning the duty cycle, the system ensures that the input voltage VPV operates at the maximum power point voltage (VMPP) of the PV arrays. This means that the duty cycle is adjusted to match the PV arrays' optimal operating voltage.

The constant output voltage, VDC, shown in Figure 9, serves as the input voltage for the inverter. An inverse proportion relationship exists between the duty cycle and the voltage VPV. Increasing the duty cycle, d, decreases the voltage input (VPV), while decreasing the duty cycle increases the voltage input. This relationship allows for precise control over the voltage input to the system. To achieve the desired voltage input, feedback control is employed. The feedback control system continuously monitors the input voltage VPV and adjusts the duty cycle accordingly to maintain the desired voltage level. This feedback loop ensures that the PV system operates at the preferred voltage input, optimizing its performance and power generation capabilities.

The MPPT (Maximum Power Point Tracking) algorithm plays a crucial role in regulating the activities of the DC-DC converter to ensure that the photovoltaic (PV) strings operate at their maximum power point (MPP). Figure 10 depicts the implementation of the incremental conductance method for MPPT. The MPP is continuously monitored by comparing the instantaneous conductance (I/V) with the incremental conductance ($\Delta I/\Delta V$). This comparison allows the MPPT algorithm to track the optimal operating point of the PV system. The goal is to find a reference voltage, denoted as V*, at which the MPPT condition is achieved. In other words, the MPPT algorithm adjusts the reference voltage (V*) so that it matches the VMPP (maximum power point voltage).

By continuously analyzing the PV system's I/V and $\Delta I/\Delta V$ characteristics, the MPPT algorithm dynamically adjusts the reference voltage to maintain its operation at or near its MPP. This enables the PV system to maximize its power output by operating at the voltage where the power generation is most efficient. The incremental conductance MPPT algorithm is widely used due to its effectiveness in tracking the MPP of the PV system under varying environmental conditions such as solar irradiance and temperature. It allows the system to adapt and optimize its performance in real-time, ensuring the PV system operates at its highest power output potential.

In the overall conversion scheme, the DC-DC converter plays a crucial role in regulating the maximum power extraction from the photovoltaic (PV) modules and transferring it to the DC link. Simultaneously, the DC-AC inverter actively transmits power synchronously to the AC grid. The reference for voltage/power control is determined based on the maximum power generated by the droop control. The modelled DC-DC converter accepts the reference power P* as its input. It processes this power and converts it to another DC voltage level in the DC link, which serves as the output. This output power from the DC-DC converter is then used as the input to the DC-AC inverter, where it is transformed into calculated DC power.

Figure 11 illustrates the different current values for the PV arrays and the DC link in the conversion process. The PV arrays generate varying levels of current based on factors such as solar irradiance and temperature, while the DC link carries the current from the PV arrays to the DC-AC inverter. Figure 11 also shows the current flowing through the diode in the circuit [23]. The diode allows current flow in one direction while blocking it in the opposite direction, ensuring the proper flow of power through the conversion system. The combination of the DC-DC converter and the DC-AC inverter allows for efficient power transfer from the PV modules to the AC grid, enabling the integration of solar power into the electric power network. The control and regulation of currents and voltages at various stages ensure optimal power extraction and transmission, contributing to the overall performance and stability of the system.

The maximum power point (MPP) of the photovoltaic (PV) system is subject to change based on variations in solar irradiance, while maintaining a constant temperature of 25°C. The control system implemented in the PV system,

specifically the MPPT algorithm, ensures that it tracks and operates the PV system at its MPP. This enables the system to consistently extract the maximum available power from the PV modules under varying environmental conditions. By employing MPPT control, the PV system continuously adjusts its operating parameters, such as the duty cycle of the DC-DC converter, to maintain the PV modules' output power at the MPP. This dynamic response to changing environmental circumstances guarantees that the PV system operates at its highest efficiency and power output potential.

The output power of the PV system, which is optimized through MPPT control, is then injected into the AC grid system. This power output corresponds to the DC power generated by the PV modules and undergoes conversion and synchronization processes through the DC-DC converter and the DC-AC inverter, respectively. By tracking the MPP and maximizing power extraction, the PV system ensures that the injected power into the AC grid system remains as close as possible to the maximum available power from the PV modules. Implementing MPPT algorithms and control mechanisms in the PV system enables it to adapt to varying environmental conditions and consistently operate at its maximum power point. This enhances the system's overall efficiency and ensures that the AC grid system receives the highest possible power output from the PV system.

The DC-AC inverter plays a crucial role in the operation of an inverter-based microgrid with a DC-DC converter. Its primary function is to synchronize with the AC grid frequency and voltage, allowing the transfer of the available solar PV power to the electric power network. In this configuration, the DC-DC converter optimizes the power generated by the solar PV system, while the DC-AC inverter efficiently injects the DC power equivalent into the AC system. The control system developed for the inverter focuses on power control, aiming to achieve stable and effective power transfer.

The control mechanism ensures that the generated power is optimized and transmitted efficiently to the AC power grid while maintaining low noise and low total harmonic distortion (THD). By regulating the inverter's output, the control system ensures that the injected power is synchronized with the AC grid and meets the required quality standards. Figure 12 illustrates the main grid voltages at the point of common coupling (PCC) and within the main network. These voltages represent the AC grid's voltage levels, which the inverter needs to synchronize with and inject power into.

Similarly, Figures 13 depict the microgrid voltages at the PCC and within the main network. These voltages represent the microgrid's voltage levels, including the interconnected renewable energy sources, storage systems, and local loads. The control system ensures that the microgrid voltages are regulated and coordinated with the main grid voltages to maintain a stable and reliable power supply. Thus, , the control system of the DC-AC inverter in the inverter-based microgrid with a DC-DC converter plays a vital role in optimizing power generation, efficiently transferring power to the AC grid, and ensuring stable and high-quality power delivery to both the main grid and the microgrid [24].

Figure 14 presents the voltage's total harmonic distortion (THD) at the point of common coupling (PCC). The THD measurement reflects the extent of distortion or harmonic content present in the three-phase voltage waveforms. A lower THD value indicates a higher quality of power and demonstrates that the developed model satisfies one of the requirements for grid-supporting operation. The quality of power injected into both the main grid and the local microgrid load is represented by Figure 14. The low THD measurement in the three-phase waveforms confirms that the control system and the inverter model effectively mitigate harmonics and ensure a clean and stable power supply.

In the three-phase grid-connected inverter-based microgrid, the grid voltage Vabc and the current Iabc are crucial AC variables used for control purposes. These variables are continuously monitored and regulated to maintain proper synchronization with the grid and provide reliable and high-quality power. Therefore, the performance and results of the inverter AC output model are evaluated based on parameters such as the grid voltage, current waveforms, and the level of THD. By effectively managing these parameters, the control system ensures optimal power injection into the main grid and the local microgrid, meeting the desired power quality standards and supporting the reliable operation of the microgrid system.

The Control System Toolbox™, power analysis functionality, is employed to compute the equivalent state-space model of the system's electrical models, built using Simscape™. This allows for the characterization of the system in terms of its state-space representation. The resulting state-space matrices are evaluated, namely A, B, C, and D. The discrete-time state-space A matrix is determined to have dimensions of 26 states by 26 states, representing the dynamics and interconnections between the system's internal states. The B matrix, representing the inputs to the system, has dimensions of 26 states by 13 inputs, indicating the control inputs and external influences on the system.

The C matrix, with dimensions of 72 outputs by 26 states, relates the system's internal states to the measured or observable outputs. Lastly, the D matrix, with dimensions of 72 outputs by 13 inputs, captures any direct feedthrough relationships between the inputs and outputs. The A matrix's eigenvalues are computed using the command $\lambda = eig(A)$ to analyze the system's stability. The eigenvalues represent the characteristic roots of the system and provide insight into its stability and behavior.

The system's eigenvalues are presented in Table 2, which lists the individual eigenvalues and their corresponding values. Additionally, Figure 15 displays a plot of the eigenvalues, visually illustrating their distribution in the complex plane. By examining the eigenvalues, one can understand the system's stability and dynamic response. The Control System Toolbox™ and Simscape™ integration enable the evaluation of the system's state-space representation and facilitate the microgrid system's analysis and control design processes.

The Control System Toolbox™, power analysis feature, is employed to compute the equivalent state-space model of

the "Proposed Secondary Control" electrical models, which are built using Simscapel™. This allows for the characterization of the system in terms of its state-space representation. The resulting state-space matrices are evaluated, namely A, B, C, and D. The discrete-time state-space A matrix is determined to have dimensions of 26 states by 26 states. This matrix represents the dynamics and interconnections between the system's internal states. The B matrix, with dimensions of 26 states by 13 inputs, represents the inputs to the system, including control inputs and external influences.

The C matrix, with dimensions of 72 outputs by 26 states, relates the system's internal states to the measured or observable outputs. Finally, the D matrix, with dimensions of 72 outputs by 13 inputs, captures any direct feedthrough relationships between the inputs and outputs. The A matrix's eigenvalues are computed using the command $\lambda = eig(A)$ to analyze the system's stability. The eigenvalues represent the characteristic roots of the system and provide insight into its stability and dynamic behavior.

The resulting eigenvalues of the system are presented in Table 2. This table lists the individual eigenvalues and their corresponding values, allowing for further analysis and interpretation of the system's stability characteristics. One can better understand the system's stability, performance, and dynamic response by evaluating the eigenvalues and analyzing their properties. The utilization of the Control System Toolbox™ and Simscapel™ enables the evaluation and analysis of the system's state-space representation, facilitating the design and optimization of the proposed secondary control system.

.

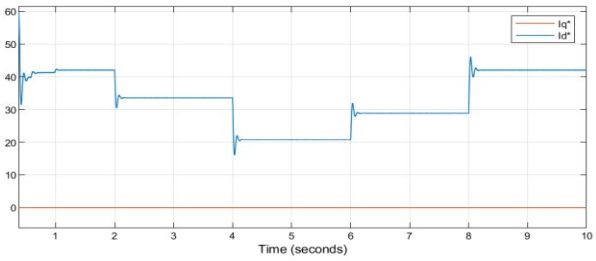

Fig. 6. The d-q current reference.

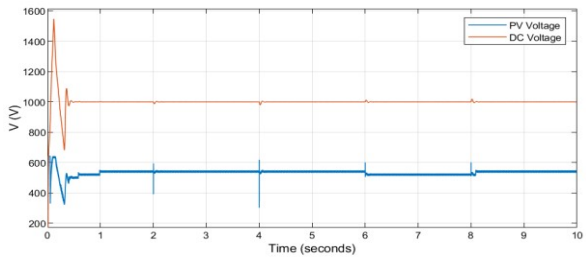

Fig. 7. Voltage at the DC link and the PV terminals.

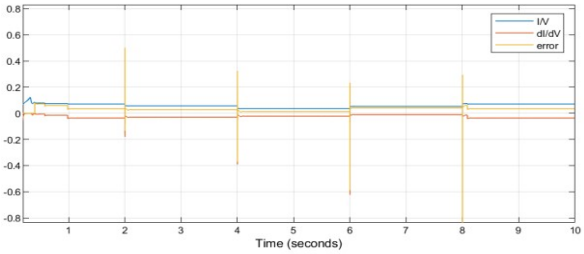

Fig. 8. MPPT instant conductance V/I, incremental conductance, MPPT Error.

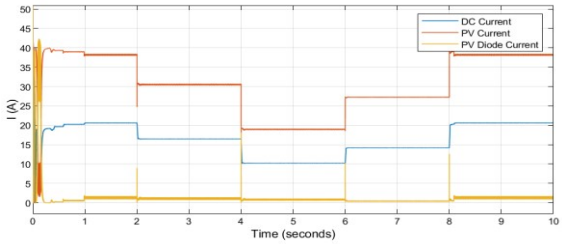

Fig. 9. PV Current, DC current and PV Diode Current.

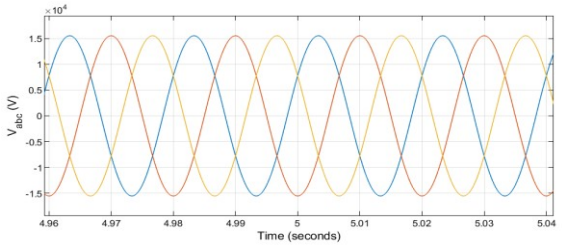

Fig. 10. Main grid Three-phase voltage waveforms.

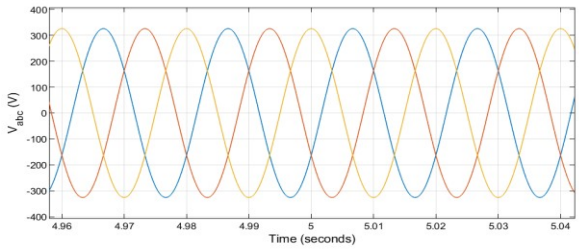

Fig. 11. Microgrid PCC Three-phase voltage waveforms

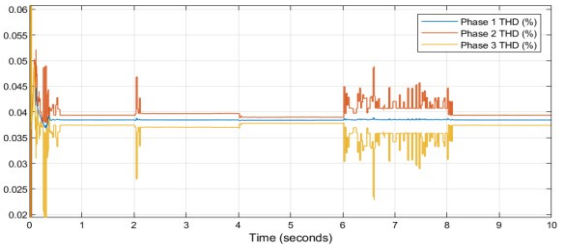

Fig. 12. AC output voltage waveform THD

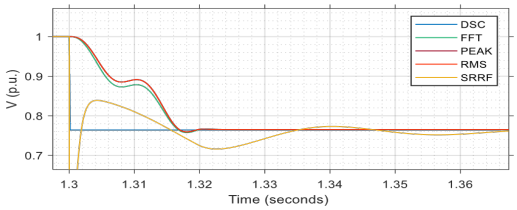

Fig. 13. DSC sag detection compared to FFT, SRRF, PEAK and RMS methods at fault inception

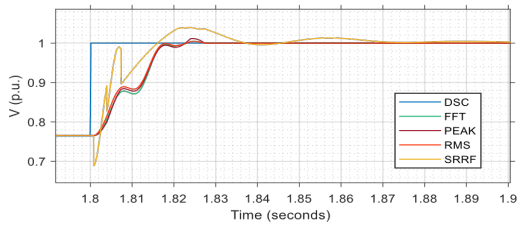

Fig. 14. DSC sag detection compared to FFT, SRRF, PEAK, and RMS methods at fault clearance

TABLE I. SAG DETECTION

Techniques	Detection Time of Fault Inception (seconds)	Detection Time of Fault Clearance (seconds)
DSC	1.3001522	1.80015210
FFT	1.3167960	1.82308800
PEAK	1.3169960	1.82274000
RMS	1.3169840	1.82309200
SRRF	1.3012721	1.81606000

TABLE II. EIGENVALUES OF THE DEVELOPED MODEL

Mode	Model	Mode	Model
λ_1	-0.6256 + 0.0000i	λ_{14}	-0.9863 + 0.0000i
λ_2	-0.4110 + 0.0000i	λ_{15}	-0.9863 + 0.0000i
λ_3	-0.4110 + 0.0000i	λ_{16}	-1.0000 + 0.0000i
λ_4	-0.2678 + 0.0000i	λ_{17}	-0.9999 + 0.0000i
λ_5	-0.9991 + 0.0000i	λ_{18}	-0.9999 + 0.0000i
λ_6	-0.9743 + 0.1131i	λ_{19}	-1.0000 + 0.0000i
λ_7	-0.9743 - 0.1131i	λ_{20}	-1.0000 + 0.0000i
λ_8	-0.9743 + 0.1131i	λ_{21}	-1.0000 + 0.0000i
λ_9	-0.9743 - 0.1131i	λ_{22}	-1.0000 + 0.0000i
λ_{10}	-0.8018 + 0.0000i	λ_{23}	-1.0000 + 0.0000i
λ_{11}	-0.8018 + 0.0000i	λ_{24}	-1.0000 + 0.0000i
λ_{12}	-0.9512 + 0.0000i	λ_{25}	-1.0000 + 0.0000i
λ_{13}	-0.9863 + 0.0000i	λ_{26}	-1.0000 + 0.0000i

5. Conclusion

This study aimed to implement an active and reactive power control system based on droop control, which is suitable for an inverter-based microgrid with a DC-DC power converter. This control scheme is particularly relevant for solar-photovoltaic systems operating in grid-supporting modes where voltage and frequency regulation is required. The droop control approach was integrated into the overall control scheme of the grid-connected PV system without compromising its design and effectiveness. The droop control was applied between the outer control loop for DC link voltage and the inner control loop for current, ensuring coordinated power control. The variation in grid frequency, represented by the difference between the actual frequency ω and the reference frequency ω*, was utilized to regulate the output power. The maximum power point (Pmpp) estimation was achieved using maximum power point tracking (MPPT) control, allowing for efficient power extraction from the PV system. In terms of active power control, the inverter's output power was determined using P-ω droop control, which mimics the inertial response of synchronous generators. This control mechanism ensures that the inverter responds to changes in grid frequency and adjusts its active power output accordingly. For reactive power control, the output of the voltage source inverter was determined using Q-E droop control. This control scheme enables the inverter to regulate its reactive power output based on the difference between actual and reference voltage. By implementing this active and reactive power control strategy based on droop control, the study successfully achieved the desired voltage and frequency regulation in the grid-supporting mode of the inverter-based microgrid. The droop control approach effectively maintained grid stability and provided the necessary power support.

Acknowledgements

Authors may acknowledge to any person, institution or department that supported to any part of study.

References

[1] E. Buraimoh and I. E. Davidson, "Overview of Fault Ride-Through Requirements for Photovoltaic Grid Integration, Design and Grid Code Compliance," *9th Int. Conf. Renew. Energy Res. Appl. ICRERA 2020*, pp. 332–336, Sep. 2020, doi: 10.1109/ICRERA49962.2020.9242914.

[2] C. Serir *et al.*, "Electrification of a load by a hybrid photovoltaic-wind system with battery storage," *11th IEEE Int. Conf. Renew. Energy Res. Appl. ICRERA 2022*, pp. 571–575, 2022, doi: 10.1109/ICRERA55966.2022.9922812.

[3] A. Q. Al-Shetwi, M. Z. Sujod, and F. Blaabjerg, "Low voltage ride-through capability control for single-stage inverter-based grid-connected photovoltaic power plant," *Sol. Energy*, vol. 159, no. November 2017, pp. 665–681, 2018, doi: 10.1016/j.solener.2017.11.027.

[4] B. N. Reddy *et al.*, "Switched Quasi Impedance-Source DC-DC Network for Photovoltaic Systems," *Int. J. Renew. Energy Res.*, vol. 13, no. 2, pp. 681–698, Jun. 2023, doi: 10.20508/IJRER.V13I2.14097.G8740.

[5] A. Arzani and G. K. Venayagamoorthy, "Computational approach to enhance performance of photovoltaic system inverters interfaced to utility grids," *IET Renew. Power Gener.*, vol. 12, no. 1, pp. 112–124, 2018, doi: 10.1049/iet-rpg.2016.1044.

[6] Y. Yang, K. A. Kim, F. Blaabjerg, and A. Sangwongwanich, "PV system modeling, monitoring, and diagnosis," *Adv. Grid-Connected Photovolt. Power Convers. Syst.*, pp. 45–74, 2019, doi: 10.1016/b978-0-08-102339-6.00003-8.

[7] K. Ishaque, Z. Salam, H. Taheri, and Syafaruddin, "Modeling and simulation of photovoltaic (PV) system during partial shading based on a two-diode model," *Simul. Model. Pract. Theory*, vol. 19, no. 7, pp. 1613–1626, 2011, doi: 10.1016/j.simpat.2011.04.005.

[8] M. Uzunoglu, O. C. Onar, and M. S. Alam, "Modeling, control and simulation of a PV/FC/UC based hybrid power generation system for stand-alone applications," *Renew. Energy*, vol. 34, no. 3, pp. 509–520, 2009, doi: 10.1016/j.renene.2008.06.009.

[9] S. R. Madeti and S. N. Singh, "Modeling of PV system based on experimental data for fault detection using kNN method," *Sol. Energy*, vol. 173, no. March, pp. 139–151, 2018, doi: 10.1016/j.solener.2018.07.038.

[10] N. Akoubi, J. Ben Salem, and L. El Amraoui, "Combination of artificial neural network-based approaches to control a grid-connected photovoltaic source under partial shading condition," *Int. J. Renew. Energy Res.*, vol. 13, no. 2, pp. 778–789, Jun. 2023, doi: 10.20508/IJRER.V13I2.13530.G8753.

[11] F. Blaabjerg, Y. Yang, D. Yang, and X. Wang, "Distributed Power-Generation Systems and Protection," *Proc. IEEE*, vol. 105, no. 7, pp. 1311–1331, 2017, doi: 10.1109/JPROC.2017.2696878.

[12] T. Suntio and A. Kuperman, "Comments on 'An efficient partial power processing DC/DC converter for distributed PV architectures,'" *IEEE Trans. Power Electron.*, vol. 30, no. 4, p. 2372, Apr. 2015, doi: 10.1109/TPEL.2014.2327018.

[13] Q. Lv, J. Zhang, K. Ding, Z. Zhang, H. Zhu, and R. Hou, "The Output Power Smoothing Method and Its Performance Analysis of Hybrid Energy Storage System for Photovoltaic Power Plant," *10th IEEE Int. Conf. Renew. Energy Res. Appl. ICRERA 2021*, pp. 36–39, 2021, doi: 10.1109/ICRERA52334.2021.9598777.

[14] M. Amir Aziat Bin Ishak, A. Ibrahim, K. Sopian, M. Faizal Fauzan, M. Aqil Afham Rahmat, and A. Sufiyan Abd Hamid, "Heat Transfer Performance of a Novel Circular Flow Jet Impingement Bifacial Photovoltaic Thermal PVT Solar Collector," *Int. J. Renew. Energy Res.*, vol. 13, no. 2, pp. 818–830, Jun. 2023, doi: 10.20508/IJRER.V13I2.13886.G8756.

[15] H. Choi, M. Ciobotaru, M. Jang, and V. G. Agelidis, "Performance of Medium-Voltage DC-Bus PV System Architecture Utilizing High-Gain DC-DC Converter," *IEEE Trans. Sustain. Energy*, vol. 6, no. 2, pp. 464–473, Apr. 2015, doi: 10.1109/TSTE.2014.2382690.

[16] E. Buraimoh and I. E. Davidson, "Fault Ride-Through Analysis of Current- and Voltage-Source Models of Grid Supporting Inverter-Based Microgrid," *IEEE Can. J. Electr. Comput. Eng.*, vol. 44, no. 2, pp. 189–198, Jun. 2021, doi: 10.1109/ICJECE.2020.3035036.

[17] R. Alkassem, M. Al Ahmadi, and A. Draou, "Modeling and simulation analysis of a hybrid PV-wind renewable energy sources for a micro-grid application," *9th Int. Conf. Smart Grid, icSmartGrid 2021*, pp. 103–106, Jun. 2021, doi: 10.1109/ICSMARTGRID52357.2021.9551215.

[18] E. Buraimoh, I. E. Davidson, and F. Martinez-Rodrigo, "Decentralized Fast Delayed Signal Cancelation Secondary Control for Low Voltage Ride-Through Application in Grid Supporting Grid Feeding Microgrid," *Front. Energy Res.*, vol. 0, p. 86, Apr. 2021, doi: 10.3389/FENRG.2021.643920.

[19] D. Ramirez, F. Martinez-Rodrigo, S. de Pablo, and L. Carlos Herrero-de Lucas, "Assessment of a non linear current control technique applied to MMC-HVDC during grid disturbances," *Renew. Energy*, vol. 101, pp. 945–963, Feb. 2017, doi: 10.1016/J.RENENE.2016.09.050.

[20] E. Buraimoh, I. E. Davidson, and F. Martinez-Rodrigo, "Fault ride-through enhancement of grid supporting inverter-based microgrid using delayed signal cancellation algorithm secondary control," *Energies*, vol. 12, no. 20, pp. 7–8, 2019, doi: 10.3390/en12203994.

[21] A. Ravi, P. S. Manoharan, and J. Vijay Anand, "Modeling and simulation of three phase multilevel inverter for grid connected photovoltaic systems," *Sol. Energy*, vol. 85, no. 11, pp. 2811–2818, 2011, doi: 10.1016/j.solener.2011.08.020.

[22] A. M. Colak, Y. Tawada, R. Inzunza, and T. Ambo, "Evaluation of Interoperability Functions via Modbus-TCP for Photovoltaic Inverters," *10th IEEE Int. Conf. Renew. Energy Res. Appl. ICRERA 2021*, pp. 111–115, 2021, doi: 10.1109/ICRERA52334.2021.9598491.

[23] T. Ishiyama, "Indoor Photovoltaic Energy Harvesting and Power Management for IoT Devices," *11th IEEE Int. Conf. Renew. Energy Res. Appl. ICRERA 2022*, pp. 461–464, 2022, doi: 10.1109/ICRERA55966.2022.9922863.

[24] F. Selim, T. F. Megahed, M. Aly, M. Shoyama, and S. M. Abdelkader, "Model Predictive Control Based Improved Techno-Economic Control Strategy for Photovoltaic-Battery Microgrids," *11th IEEE Int. Conf. Renew. Energy Res. Appl. ICRERA 2022*, pp. 230–235, 2022, doi: 10.1109/ICRERA55966.2022.9922814.